

Image Quality Impact of SmartGrid Processing in Bedside Chest Imaging

Authors: Lori L. Barski (MS), Dong Yang (Ph.D.), Mary Couwenhoven (MS)

Introduction

Scattered radiation is known to degrade image quality in diagnostic X-ray imaging. Traditional methods of reducing scatter are collimation, utilizing an air-gap, and/or utilizing an anti-scatter grid [1]. Best practices in radiography prescribe collimation on every exam [2] and, while this is helpful, it is not completely sufficient due to scatter that occurs within the patient. Likewise, air-gap techniques are helpful [1], but are not practical at the bedside. Anti-scatter grids are by far the most popular means of reducing scatter in portable imaging, but they present challenges to radiographers (e.g., positioning and alignment) and increases dose to the patient [1,3].

A new image processing tool, SmartGrid, has been developed that compensates for the effects of X-ray scatter in an image, and produces results comparable to those of a physical anti-scatter grid. Figure 1 shows a pair of portable chest images captured with a grid (top left), without a grid (top right), and the results with SmartGrid (bottom left).

The scatter distribution image (bottom right) demonstrates regions of the image that are most impacted by scatter (lighter tone). SmartGrid processing estimates the scatter distribution and removes it, resulting in an image with improved contrast. Many physical factors affect scatter: energy spectrum of the beam, thickness and material composition of the object, and collimation, to name a few. SmartGrid accommodates these variables automatically and results in image quality that approximates anti-scatter grid visual performance.

The SmartGrid Algorithm

The SmartGrid algorithm (Figure 2) is an enhancement algorithm that improves image contrast by suppressing scatter in the image. The fundamental concept is one of developing a scatter distribution image, which is a representation of the scatter contained in the image, and then subtracting it from the original input image.

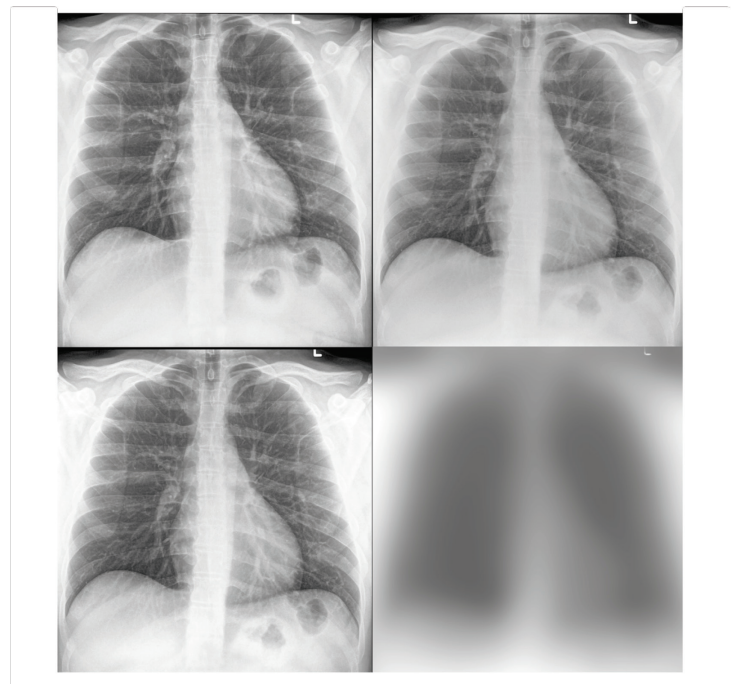


Figure 1. Portable chest exam captured with a grid (top left) and without a grid (top right, grid exposure 1.25X non-grid), and then processed with SmartGrid (bottom left) with the corresponding scatter distribution image (bottom right).

The scatter distribution image is developed using information from the image in both linear exposure space as well as attenuation space, which is a log transformation of the linear data. Segmentation is done to focus the development of the scatter field on relevant anatomical data and is used to compute the mean linear exposure of the input image. Parameters used to estimate scatter are determined. These include the scatter-to-primary ratio (SPR) and a curvature parameter used to control perturbation of the scatter distribution as the scatter field is developed.

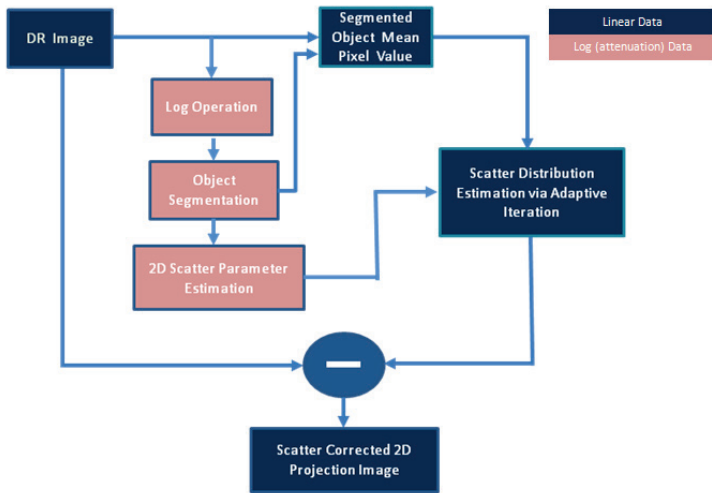


Figure 2. Flow diagram of the SmartGrid algorithm.

The scatter distribution image is computed based upon the assumption that every object exposed by X-rays has a basic scatter distribution that is characterized by a certain level of energy and scatter intensity variation across the whole object field of view. Adaptive updating of the scatter intensity across the entire object field of view is performed in a repetitive fashion based upon the SPR parameter for a prescribed number of iterations.

SmartGrid Image Quality

In order to assess the image quality impact of SmartGrid processing, a clinical study evaluating paired grid and non-grid portable chest images was conducted at the University of

Rochester Medical Center with IRB oversight. Patients and healthy volunteers, under informed consent and who met the inclusion criteria (age greater than 18, body mass index greater than 25 and a chest circumference greater than 90 cm, non-pregnant females, and no history of high-radiation exposure), had portable chest exams taken with and without anti-scatter grids. Grid/non-grid usage was alternated for in-patient subjects over a time span of days, whereas healthy volunteers were imaged within a time span of minutes. Techniques were selected and documented by the radiographer at the time of the exam, following department guidelines for the site's standard of care.

Two sets of pair-wise comparisons were evaluated (side-by-side) for each grid/non-grid image pair: SmartGrid (SG) vs. Grid (n=44) and SmartGrid vs. standard default processing (EVP Plus processing available in V5.7, n=44). Pairs were presented on a PACS in randomized order to five board-certified thoracic radiologists (3 - 57 yrs. experience) and anatomical regions (retro-cardiac, carina/airways, sub-diaphragm, chest wall, and lung parenchyma) were rated using a +/- 3 point preference scale. For each pair, the reader picked the image with the best region (e.g., retro-cardiac) and rated it as +/- 0, 1, 2, or 3, where the sign indicated the left or right monitor (i.e., left-preferred was indicated with negative numbers) and the magnitude corresponded to the degree of clinical impact (Table 1). Readers were free to pan, zoom, and adjust window width and window level as desired. Upon completion of the reader study, response data was decoded such that positive values indicated preference in favor of SmartGrid.

Additionally, each image of the pair was rated for diagnostic quality using a 4-point RadLex scale [4] (Table 2), allowing decimal ratings (e.g., 3.3) between the integer anchors.

	Score	Definition	
Left Preferred	-3	Image displayed on left is strongly preferred	Clinical Impact
	-2	Image displayed on left is moderately preferred	
	-1	Image displayed on left is slightly preferred	
	0	No preference between the images	No Clinical Impact
Right Preferred	1	Image displayed on right is slightly preferred	Clinical Impact
	2	Image displayed on right is moderately preferred	
	3	Image displayed on right is strongly preferred	

Table 1. Preference rating scale.

Score	Term	Definition
1	Non-diagnostic	Unacceptable for diagnostic purposes. Little or no clinically-usable diagnostic information (e.g., gross underexposure or extensive motion artifact) and should be repeated.
2	Limited	Acceptable, with some technical defect (motion artifact, body habitus/poor X-ray penetration, or patient positioning, but still adequate for diagnostic purposes).
3	Diagnostic	Image quality that would be expected routinely when imaging cooperative patients.
4	Exemplary	Good, most adequate for diagnostic purposes. Image quality that can serve as an example that should be emulated.

Table 2. Diagnostic quality RadLex rating scale.

Clinical Study Results

On average, no significant overall preference difference was detected between the SmartGrid and anti-scatter grid pairs (mean difference = 0.0, 95% CI [-0.12, 0.12], p =0.941) with an average grid dose factor of 2.1x (i.e., SmartGrid exposures

were, on average, acquired with approximately half of the grid dose). Figure 3 is an example of SmartGrid processing (left) compared to the grid image (right), which was acquired at approx 3.5x the SmartGrid dose. The average overall preference difference was 1.0. Table 3 summarizes the pairwise preference differences for the anatomical regions.

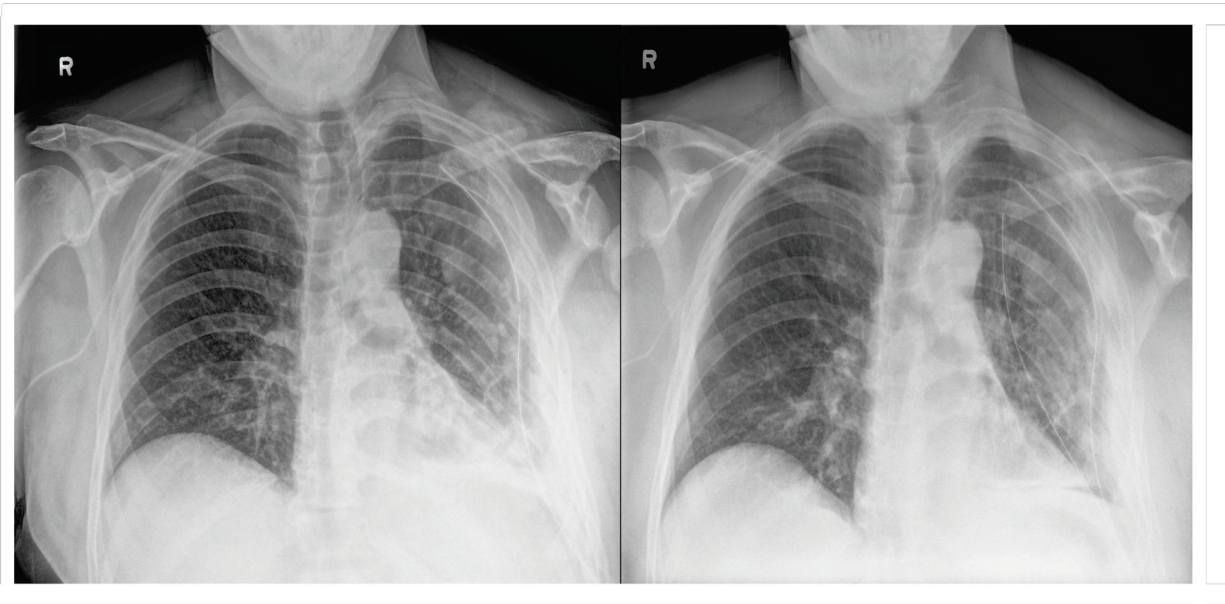


Figure 3. SmartGrid image (left): 95 kVp, 2.5 mAs, 61 in. SID, compared to grid image (right): 110 kVp, 4 mAs, 58 in. SID. Average overall preference difference is 1.0.

Grid vs. SG Preference	Mean Difference	Confidence Interval	p-value	Conclusion
Over All	0.0	-0.12, 0.12	0.941	No difference
Retrocardiac	-0.2	-0.28, -0.05	0.007*	In favor of grid
Carina/Airways	-0.2	-0.29, -0.06	0.003*	In favor of grid
Subdiaphragm	-0.1	-0.18, 0.04	0.186	No difference
Chest Wall	0.1	0.04, 0.23	0.004*	In favor of SG
Parenchyma	0.1	-0.29, 0.17	0.170	No difference

Table 3. SmartGrid vs. Grid Preference rating results (* indicates statistical significance at an alpha risk of 5%).

White Paper | SmartGrid

The difference in diagnostic quality ratings of SmartGrid vs. grids was significant in favor of SmartGrid processing (mean difference = 0.03, 95% CI [0.00, 0.05], $p = 0.044$).

Not surprising, is the result that the SmartGrid processing has significantly higher preference overall compared to images without SmartGrid enhancement (mean difference = 0.8, 95% CI [0.69, 0.84], $p < 10^{-3}$) as well as for all anatomical regions (all p -values $< 10^{-3}$).

Likewise, diagnostic quality differences were significantly in favor of SmartGrid ($p < 10^{-3}$).

Figure 4 illustrates a typical chest wall appearance as seen in a SmartGrid (left) image and the corresponding grid image (right). Scatter in this region has the potential to reduce the visualization of the pleura and the bony structures of the outer rib cage.

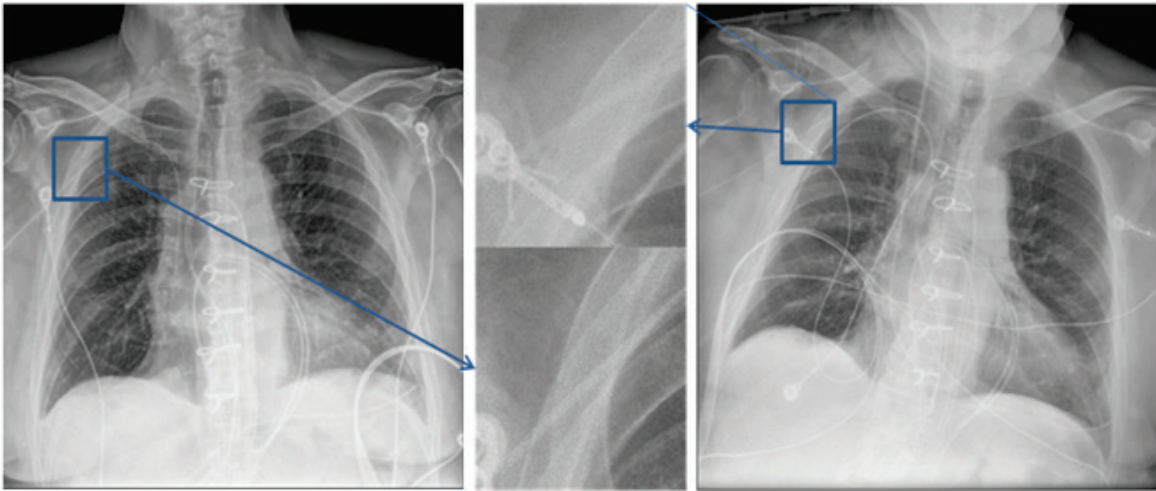


Figure 4. Chest wall example. SmartGrid (Left): 90 kVp, 2.6 mAs, 60 in. SID; Grid (right): 110 kVp, 4 mAs, 68 in. SID.

Figure 5 demonstrates the retrocardiac region of a SmartGrid image (left) and grid (right) pair. The apparent lack of contrast in the grid image is likely caused by grid misalignment, illustrating exactly why a software solution to scatter compensation is of great benefit in the ICU.

Figure 6 is another portable chest comparison with the SmartGrid processing on the right, default processing of the same image without SmartGrid enabled, and the grid exposure shown on the right. Note that the non-grid image was acquired at approximately half of the grid exposure.

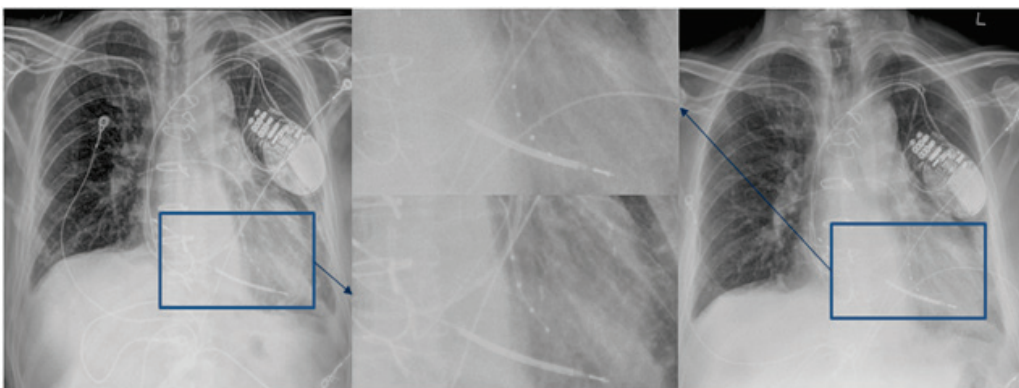


Figure 5. Retrocardiac example. SmartGrid (left): 95 kVp, 3.2 mAs, 72 in. SID; Grid (right) 112 kVp, 7.2 mAs, 72 in. SID.

White Paper | SmartGrid

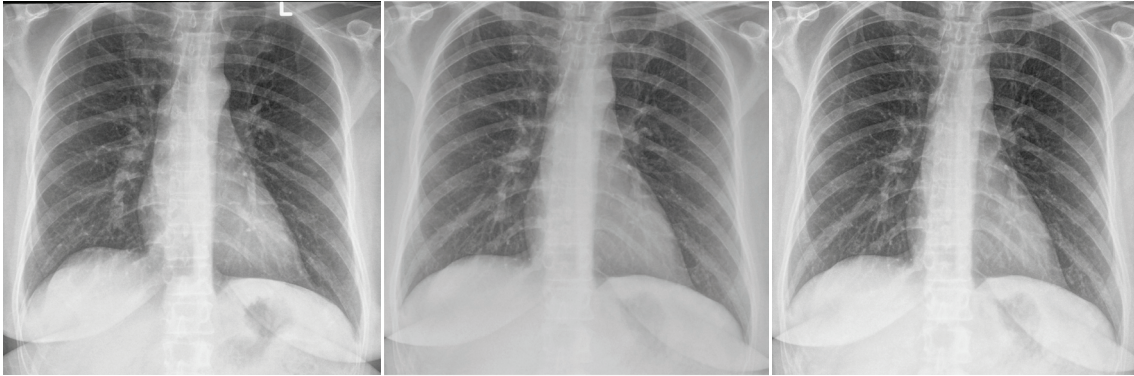


Figure 6. SmartGrid (left, 95 kVp, 2.2 mAs, 65 in. SID) and processing without SmartGrid (middle) compared to grid (right, 105 kVp, 3.2 mAs, 65 in. SID).

Conclusion

SmartGrid processing provides image quality comparable to images acquired with an anti-scatter grid at a reduced patient dose in bedside chest imaging. The benefits of grid-like image quality without the use of an anti-scatter grid can lead to improved work flow and ease of imaging for radiographers, producing a win-win for a busy hospital.

References

- ¹ Christensen, Edward E., et al. *Christensen's Physics of Diagnostic Radiology*. Lea & Febiger, 1990.
- ² T.L. Herrmann, T. L. Fauber, et. al. "Best Practices in Digital Radiography." (2012) (https://www.asrt.org/docs/default-source/publications/whitepapers/asrt12_bstpracdigradwhp_final.pdf).
- ³ J. C. Wandtke, "Bedside Chest Radiography," *Radiology*, 190:1-10 (1994).
- ⁴ Radiological Society of North America (2010) RadLex: a lexicon for uniform indexing and retrieval of radiology information resources. Available via <http://www.rsna.org/radlex/>. Accessed 22 Oct 2010.